JACS
JOURNAL OF THE AMERICAN CHEMICAL SOCIETY

Article

pubs.acs.org/JACS

Regulation of the P450 Oxygenation Cascade Involved in Glycopeptide Antibiotic Biosynthesis

Madeleine Peschke,[†,#] Kristina Haslinger,[†,#,∥] Clara Brieke,[†] Jochen Reinstein,[†] and Max J. Cryle*[,†,‡,§]

[†]Department of Biomolecular Mechanisms, Max Planck Institute for Medical Research, Jahnstrasse 29, 69120 Heidelberg, Germany
[‡]EMBL Australia, Monash University, Clayton, Victoria 3800, Australia
[§]The Department of Biochemistry and Molecular Biology and ARC Centre of Excellence in Advanced Molecular Imaging, Monash University, Clayton, Victoria 3800, Australia

Supporting Information

ABSTRACT: Glycopeptide antibiotics (GPAs) are nonribosomal peptides rich in modifications introduced by external enzymes. These enzymes act on the free peptide aglycone or intermediates bound to the nonribosomal peptide synthetase (NRPS) assembly line. In this process the terminal module of the NRPS plays a crucial role as it contains a unique recruitment platform (X-domain) interacting with three to four modifying Cytochrome P450 (P450) enzymes that are responsible for cyclizing bound peptides. However, whether these enzymes share the same binding site on the X-domain and how the order of the cyclization steps is orchestrated has remained elusive. In this study we investigate the first two reactions in teicoplanin aglycone maturation catalyzed by the enzymes $OxyB_{tei}$ and $OxyA_{tei}$. We demonstrate that both enzymes interact with the X-domain via the identical interaction site with similar affinities, irrespective of the peptide modification stage, while their catalytic activity is restricted to the correctly cross-linked peptide. On the basis of steady state kinetics of the $OxyB_{tei}$-catalyzed reaction, we propose a model for P450 recruitment and peptide modification that involves continuous association/dissociation of the P450 enzymes with the NRPS, followed by specific recognition of the peptide cyclization state by the P450 (scanning). This leads to an induced conformational change that enhances the affinity of the enzyme/substrate complex and initiates catalysis; product release then occurs, with the product itself becoming the substrate for the second enzyme in the pathway. This model rationalizes our experimental findings for this complex enzyme cascade and provides insights into the orchestration of the sequential peptide tailoring reactions on the terminal NRPS module in GPA biosynthesis.

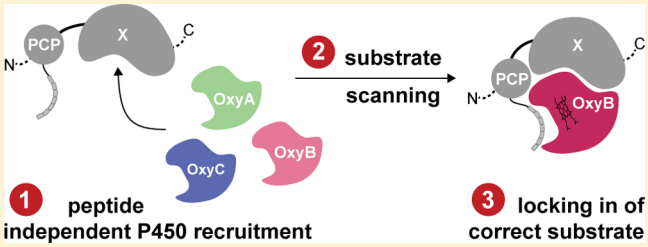

INTRODUCTION

Nonribosomal peptides are a group of structurally diverse and complex compounds possessing a wide range of biological activities, many of which have medical relevance.[1,2] The peptide core structure of these compounds is produced by mega-enzyme complexes known as nonribosomal peptide synthetases (NRPSs).[3] Such machineries are built from repetitive units of three key domains—together defined as a module—important for amino acid recognition/activation (adenylation/A-domain), peptide bond formation (condensation/C-domain) and the attachment of the peptide intermediates to the machinery (peptidyl carrier protein/PCP-domain) via a phosphopantetheinyl (Ppant) moiety, an essential posttranslational modification of the PCP-domain.[4] In the simplest (Type I) NRPS systems the modules are organized in a linear fashion with one module incorporating one amino acid.[5] However, compounds produced by a Type I NRPS can display great complexity, such that the final product often bears little resemblance to the initial peptide scaffold. One of the reasons is that NRPSs—in contrast to ribosomes—are able to incorporate a range of amino acids extending far beyond standard proteinogenic amino acids.[6,7] Furthermore, the peptide core can undergo extensive modifications: additional internal NRPS domains as well as external tailoring enzymes can catalyze the installation of many modifications.[4,8] Tailoring in *cis* is enabled through the incorporation of modifying domains into the NRPS modules by domain insertion (e.g., epimerization domains[9]), integration into a core domain (e.g., A-domains interrupted by oxidation domains[10]) or by domain-replacement (cyclization domains instead of C-domains[11]). Further structural diversity is achieved during thioesterase domain (Te-domain)-catalyzed peptide release, which often involves macrocyclization or dimerization of the precursor peptide instead of hydrolysis.[12] On the other hand, rather simple Type I NRPS assembly lines with few modification domains are also able to yield complex natural products. Important examples are the glycopeptide antibiotics where tailoring in *cis* is limited to amino acid epimerization.[13] The best known-members of this group are vancomycin (a Type I GPA) and teicoplanin (a Type IV GPA), both in clinical use against serious Gram-positive bacterial infections.[14] While the NRPS involved in GPA production yields the linear

Received: January 10, 2016
Published: May 23, 2016

ACS Publications © 2016 American Chemical Society

DOI: 10.1021/jacs.6b00307
J. Am. Chem. Soc. 2016, 138, 6746−6753

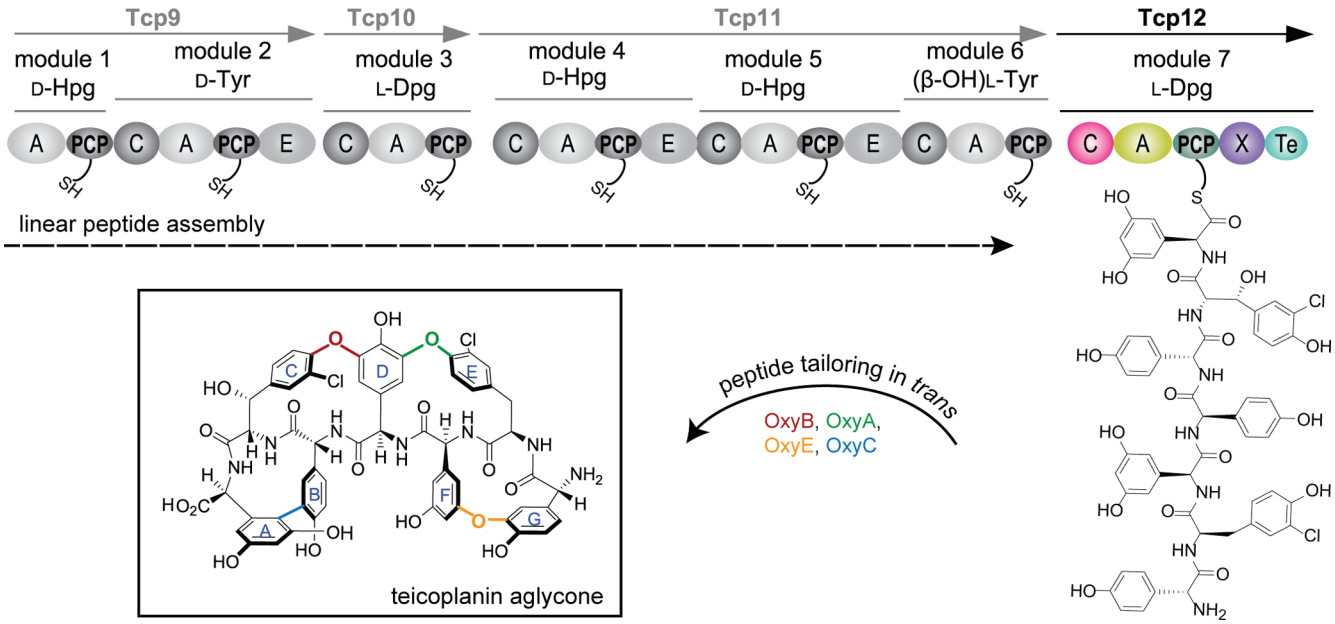

Figure 1. Biosynthesis of the teicoplanin aglycone. Sequential assembly of the linear heptapeptide by the NRPS (adenylation/A-, condensation/C-, epimerization/E-, peptidyl carrier protein/PCP- (posttranslationally modified by the attachment of a Ppant-linker), P450 recruitment/X- and thioesterase/Te-domain) followed by oxidative peptide tailoring by four P450s (OxyB, OxyA, OxyE and OxyC) acting in *trans*.

heptapeptide backbone, the complexity and diversity of GPAs is introduced by several tailoring enzymes that modify amino acids and the growing peptide co- and postsynthetically (e.g., glycosylation and methylation) (Figure 1).[15,16] One class of cosynthetic tailoring reactions is the oxidative cross-linking of aromatic amino acids in the peptide.[13] These reactions are catalyzed by Cytochrome P450 monooxygenases (P450s), resulting in a tri- or tetracyclization of the heptapeptide scaffold and the generation of the specific 3-dimensional structure crucial for GPA antibiotic activity.[11] Three of these cross-links are present in all GPA types (introduced by the enzymes OxyB, A and C), whereas the fourth cross-link (performed by OxyE) is only present in certain GPAs. In vivo and in vitro studies have shown that the P450s act in a specific order[17−19] on the precursor peptide bound to the NRPS,[20,21] most likely when it is bound to the PCP-domain of the terminal NRPS module.[22] To the best of our knowledge, this is the most complex example of multiple tailoring enzymes acting on NRPS peptide intermediates in the same NRPS module. Recent findings have demonstrated that this interaction of multiple P450s with one PCP-bound substrate requires an additional NRPS domain, known as the X-domain.[22,23] This domain—located downstream of the peptide carrying PCP-domain in the terminal NRPS module of all GPA producing NRPSs—is crucial for the peptide cross-linking reactions.[15] By effectively linking the peptide assembly to the activity of up to four external tailoring enzymes, the X-domain—itself catalytically inactive—orchestrates the introduction of several specific modifications at the same stage of NRPS-based peptide biosynthesis.

With the phenolic and aryl coupling reactions being both essential for GPA activity and at the same time highly challenging from a synthetic perspective, our aim is to further investigate the order, regulation and the reaction mechanism of the P450-dependent peptide cyclization reactions that occur in the biosynthesis of teicoplanin. In this work, we now perform a detailed investigation of the role of the essential components of the P450 substrate—the PCP-, X-domain and the peptide in different cross-linking states—in the recruitment process. Furthermore, we show that the crucial P450 oxygenases are recruited via the same site on the X-domain surface and directly compete for this binding site. Lastly, by means of substrate binding experiments and kinetic studies with OxyB and OxyA enzymes, we propose a model for the orchestration of the P450 cascade in GPA biosynthesis.

RESULTS AND DISCUSSION

Oxy Enzymes Display Different Selectivity for Altered Peptide Stereochemistry. The activity of P450 (Oxy) enzymes involved in GPA production can be assessed in vitro: we have previously established a coupled turnover protocol capable of generating bicyclic peptide products that allowed us to analyze the selectivity of $OxyA_{tei}$.[22,23] These studies employed a diastereomeric mixture of teicoplanin-like heptapeptide **1** (L-Hpg or D-Hpg at the seventh position, Figure 2) that was loaded from the corresponding peptidyl-CoAs onto the PCP-domains using the phosphopantheteinyl transferase Sfp from *Bacillus subtilis*;[24] epimerization of the C-terminal Hpg-residue is currently unavoidable during synthesis.[21,23] Since only ~40% of monocyclic peptide **2** was cross-linked by $OxyA_{tei}$ to form the bicyclic peptide **3**, we sought to clarify the stereoselectivity of $OxyA_{tei}$.[22,23] Through careful comparison of the HPLC/MS traces of $OxyB_{tei}$ turnover with those of the coupled $OxyB_{tei}$-$OxyA_{tei}$ assay, we deduced that only one of the diastereomers of **2**-D/L was efficiently converted into **3** (SI Figure S3). To elucidate the impact of the peptide stereochemistry on turnover, further efforts were made to purify the diastereomers by preparative HPLC to afford **1**-L (L-Hpg_7) and **1**-D (D-Hpg_7) (Figure 2, see Methods, SI Figure S1, S2). Coupled turnover experiments with these substrates clearly showed that while $OxyB_{tei}$ activity is independent of the stereochemistry of the seventh amino acid in **1**, $OxyA_{tei}$ strongly favors the natural L-configuration of its monocylic substrate **2** (Figure 3a, SI Figure S4 and Table S1).

DOI: 10.1021/jacs.6b00307
J. Am. Chem. Soc. 2016, 138, 6746−6753

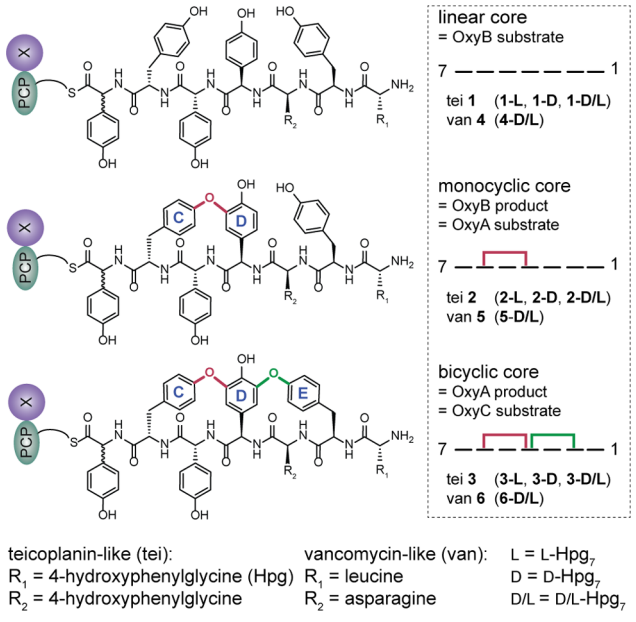

Figure 2. *Peptidyl*-PCP-X substrates and products used in this study: these also include diastereomerically enriched samples of **1**-L and **1**-D.

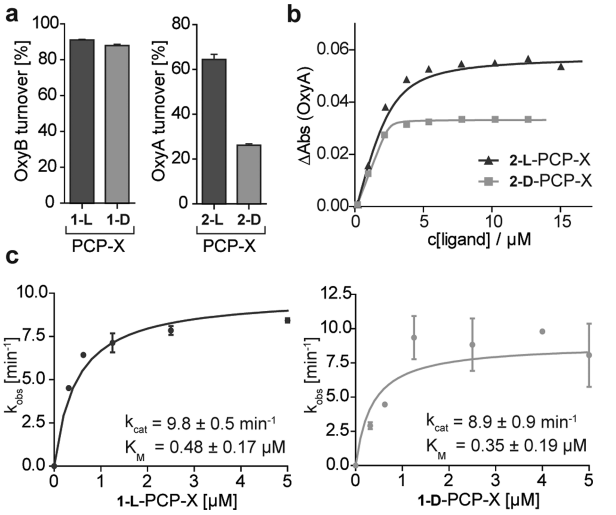

Figure 3. Stereoselectivity of $OxyB_{tei}$ and $OxyA_{tei}$ toward the seventh amino acid in the peptide. (a) Coupled $OxyB_{tei}$/$OxyA_{tei}$ in vitro activity studies with linear **1**-L and **1**-D-PCP-X. (b) Spectral response (extrapolated ΔAbs, see Methods) of $OxyA_{tei}$ upon binding of the monocyclic **2**-L and **2**-D-PCP-X. (c) Steady state kinetics of $OxyB_{tei}$ with linear **1**-L and **1**-D-PCP-X.

On the basis of these results, we tested whether the selectivity of $OxyA_{tei}$ can be observed in substrate binding: we assessed this by measuring the effect of increasing substrate concentrations on the P450 spin state using UV−visible spectroscopy. Therefore, we established a modified $OxyB_{tei}$ turnover protocol with subsequent NADH removal to generate the $OxyA_{tei}$ substrate **2** (see Supporting Methods). Using the monocyclic L- and D-diastereomeric peptides (**2**-L and **2**-D) in our titrations, we indeed observed the strongest binding response for **2**-L, which is in accordance to the preference of $OxyA_{tei}$ for this peptide (Figure 3b, SI Figure S5, Table S2). From these experiments we conclude that while $OxyB_{tei}$ is tolerant of altered stereochemistry of the seventh amino acid of the peptide, $OxyA_{tei}$ is not. This shows that a higher degree of cyclization and thus three-dimensional complexity of the substrate peptide correlates with increasing Oxy selectivity in the cascade;[3] as a result, we generally focus on substrates **1** and **2** bearing the natural L-configuration of the seventh amino acid in the following experiments.

Oxidation Kinetics Implicate Heptapeptides as the In Vivo Substrates of the Oxy Cascade. Next, we analyzed whether $OxyB_{tei}$ displays a preference for **1**-L that cannot be seen in turnover end point measurements: thus, we analyzed the kinetic parameters of $OxyB_{tei}$ with **1**-L and **1**-D coupled to PCP-X as substrates (Figure 3c, SI Figures S6−S8, Table S3). For both peptides we obtained comparable values for K_M and k_{cat}, demonstrating equal acceptance by $OxyB_{tei}$. In addition, we also analyzed the well-studied OxyB homologue from the vancomycin system ($OxyB_{van}$). Using a vancomycin-like heptapeptide **4**-D/L coupled to the PCP-X from the vancomycin system as a substrate (Figure 2), we observed that the kinetic parameters for peptide cyclization (K_M < 0.1 µM, k_{cat} 43.7 ± 2.0 min^{-1}) were superior to $OxyB_{tei}$ (SI Figures S6−S8, Table S3), which is in accordance with previous results showing this enzyme to be both highly efficient and promiscuous toward a broad range of substrates.[20,21,25−27] These kinetic parameters were also dramatically improved over those reported for PCP-bound hexapeptides (K_M = 4−13 µM, k_{cat} = 6.7 min^{-1}).[21] The dramatic increase in substrate affinity and turnover velocity observed for $OxyB_{van}$ in the presence of the X-domain strongly supports peptide cyclization of heptapeptides bound to the final NRPS module as opposed to hexapeptide cyclization in vivo − a much-debated question in the field.[17−20,28−30]

Loading State of the PCP Tunes Oxy Affinity for the NRPS. Having again demonstrated the importance of the X-domain for efficient peptide cross-linking, we investigated the role of the individual NRPS substrate components (peptide, PCP- and X-domain) in P450 binding. Thus, we determined the binding affinity of the X-domain alone as well as the PCP-X didomain in different PCP modification states, *apo*- (unloaded PCP), *holo*- (PCP loaded with Ppant-linker) and *peptidyl*-PCP (**1**-L)), to $OxyB_{tei}$ using UV−visible spectroscopy. In order to determine the dissociation constants (K_D) for the otherwise spectroscopically silent peptide-free variants, we employed a competitive equilibrium system: binding events are visualized through displacement of bound **1**-L-PCP-X from $OxyB_{tei}$ and quantified using global data analysis (see Methods and SI) (Table 1, SI Figure S9). Using this setup, we observed that the X-domain displays >2-fold higher affinity to $OxyB_{tei}$ than the

Table 1. Results of UV−Visible Spectroscopic Assays of *Peptidyl*-PCP-X (1-L), *apo*/*holo*-PCP-X Didomain and X-Domain to $OxyB_{tei}$[a]

1-L-/*apo*-/*holo*-PCP-X or X binding to $OxyB_{tei}$					
K_D [µM]	value	SE	mean	min	max
1-L-PCP-X	1.66	0.12	1.66	1.31	2.11
X-domain	6.02	0.50	6.04	4.69	7.75
PCP-X, *apo*	13.22	1.02	13.26	10.00	17.03
PCP-X, *holo*	14.73	1.33	14.78	11.52	18.99

[a]Global data analysis of a competitive equilibrium system with different interaction partners. Values for K_D were fitted with the program Dynafit[37] (see SI) with corresponding Standard Error (SE). A robust nonlinear uncertainty assessment was obtained from Monte Carlo analysis (min, max define uncertainty interval, 1000 iterations).

DOI: 10.1021/jacs.6b00307
J. Am. Chem. Soc. 2016, 138, 6746−6753

PCP-X didomain protein (*apo* or *holo*); however, the additional presence of the peptide increases the affinity of the PCP-X construct (**1**-L-PCP-X), leading to a > 4-fold higher affinity to $OxyB_{tei}$ compared to the X-domain alone.

These results indicate that the X-domain is the initial driving force for the recruitment of the P450s to the peptide, whereas the presence of the PCP-domain—shown to be sufficient and essential for the substrate presentation to P450s in other systems[21,31−36]—actually reduces the affinity of the NRPS to $OxyB_{tei}$. In the context of the entire NRPS machinery this may be an important property to ensure that the tailoring P450s do not directly compete with the main assembly line for *holo*-PCP and thereby block the final coupling step. On the other hand, the interaction of *holo*-PCP with the A- and C-domains during the normal catalytic cycle of the NRPS module may free up the X-domain to interact with the P450s and thereby ensure their presence for efficient tailoring once the heptapeptide is assembled. Since the peptide appears to be necessary for an efficient interaction of the P450s with the PCP-X protein, we next focused on understanding the role of the substrate peptide in determining the order of the cross-linking reactions.

Order of the P450 Cascade Is Enforced by the Peptide Cyclization State. Previous in vivo studies indicated that OxyB introduces the first cross-link into the linear substrate peptide and that the activities of the following P450 enzymes strictly depend on the presence of the OxyB-catalyzed C-*O*-D ring in the substrate peptide (Figure 2).[17,19] We next set out to analyze the order of the oxygenation cascade in vitro by performing further UV−visible substrate binding studies with $OxyB_{tei}$ and $OxyA_{tei}$. A first set of experiments was performed with the linear **1**-L-PCP-X conjugate: this ligand was found to evoke spectral shifts in both P450s with a signature typical for substrate binding, albeit with a significantly smaller amplitude for $OxyA_{tei}$ than for $OxyB_{tei}$ (~6-fold difference in spin state shift) (Figure 4, SI Figure S5, Table S2). Curiously, the

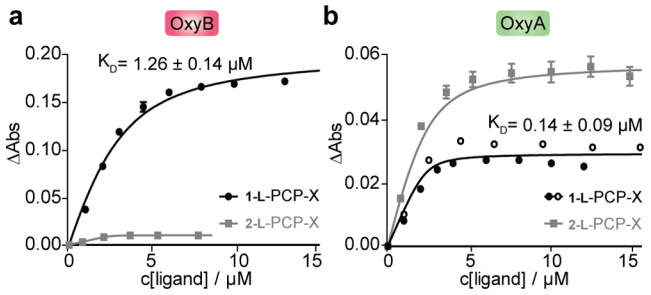

Figure 4. In vitro investigation of the order of the cross-linking reactions catalyzed by $OxyB_{tei}$ and $OxyA_{tei}$. Extrapolated amplitudes of $OxyB_{tei}$ and $OxyA_{tei}$ UV−visible spectral response (ΔAbs, see Methods) upon binding of linear (**1**-L) and monocyclic (**2**-L) *peptidyl*-PCP-X conjugates.

apparent K_D determined for $OxyA_{tei}$ is an order of magnitude smaller than for $OxyB_{tei}$: although this would suggest that $OxyA_{tei}$ can also accept linear substrate peptides for turnover, we did not observe any activity in an $OxyA_{tei}$ activity assay using **1**-L-PCP-X (SI Figure S10).

In a second set of binding experiments with the monocyclic **2**-L-PCP-X conjugate, we observed a dramatic decrease in spectral amplitude for $OxyB_{tei}$ (~20-fold) and an increase for $OxyA_{tei}$ (~2-fold) compared to the linear substrate (**1**-L-PCP-X) (Figure 4). The apparent affinities observed in these experiments are difficult to compare quantitatively, as **2** is prepared via an in vitro $OxyB_{tei}$ turnover reaction and cannot be purified from the reaction mixture. However, since the extrapolated amplitudes refer to the catalytically competent orientation of the peptide within the active site, the decreased spectral responses of $OxyB_{tei}$ toward **2** and $OxyA_{tei}$ toward **1** support $OxyA_{tei}$ as the second enzyme in the peptide-cyclization cascade. The K_D values determined for $OxyB_{tei}$ and $OxyA_{tei}$ for **1**-L-PCP-X would indicate that there must be an additional selectivity-conferring step after association of the *peptidyl*-PCP-X/P450 complex in the P450 catalytic cycle. Since the interaction of **1**-L-PCP-X with both $OxyB_{tei}$ and $OxyA_{tei}$ would furthermore suggest a direct competition of the P450s for the linear substrate, we next addressed the question whether all tailoring P450s compete for the same binding site on the X-domain.

The X-Domain Displays a Conserved Interaction Interface for the Oxy Enzymes. Previously, we showed that the three essential tailoring P450s in teicoplanin biosynthesis—$OxyB_{tei}$, $OxyA_{tei}$ and $OxyC_{tei}$—are recruited to the NRPS by the X-domain.[22] However, it remained elusive whether a single binding site on the X-domain surface mediates the recruitment of the P450 enzymes to the peptide substrate. On the basis of the crystal structure of an $OxyB_{tei}$-X-domain complex (PDB ID 4TX3), we demonstrated that this interaction is formed through rigid body docking—displaying only minor changes in the two interaction partners—and is dominated by the formation of hydrogen bonds and salt bridges.[22] The interface is formed by three main regions on the X-domain side, one of which has been shown to be crucial for the binding of $OxyB_{tei}$ and consequently for cyclization of the peptide. To test whether the other P450s also bind to the same site, three PCP-X didomain variants bearing mutations in the X-domain regions involved in $OxyB_{tei}$ recruitment were used for peptide-free coelution experiments by analytical size exclusion chromatography with $OxyA_{tei}$ and $OxyC_{tei}$. The results obtained were comparable to those shown for $OxyB_{tei}$:[22] mutations in a single region (X_1: R167A, R171A) were able to prevent the association and coelution of $OxyA_{tei}$ and $OxyC_{tei}$ with the X-domain (Figure 5, SI Figures S11/S12). In addition, both P450s, and in particular $OxyC_{tei}$, appear to bind to the other mutant variants with a slightly decreased affinity compared to the wild type PCP-X protein. Thus, $OxyB_{tei}$,

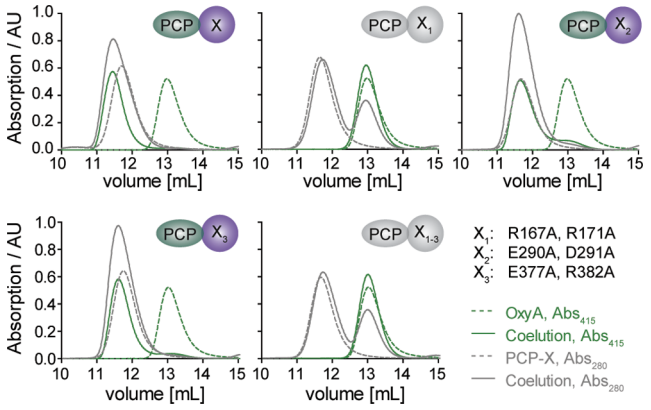

Figure 5. Analytical size exclusion chromatography of $OxyA_{tei}$ with wild type and mutant variants of the PCP-X didomain. Dashed lines: elution profile of the individual proteins, solid lines: coelution profile of a 3:1 PCP-X:$OxyA_{tei}$ mixture, with detection either at λ = 280 nm (gray) or 415 nm (heme absorption, green).

DOI: 10.1021/jacs.6b00307
J. Am. Chem. Soc. 2016, 138, 6746−6753

$OxyA_{tei}$ and $OxyC_{tei}$ do indeed share the same interaction site on the X-domain, namely the loop connecting α-4/ α-5 that forms ionic interactions with the conserved PRDD motif in the F-helix of tailoring P450s (SI Figure S13).

Oxy Enzymes Compete for the X-Domain Binding Interface. The fact that multiple P450s are recruited by the same site on the X-domain with similar binding affinities implies a competition between the P450s for the X-domain and hence for the PCP-bound substrate peptide. With this knowledge, we next investigated whether the P450s following OxyB in the oxygenation cascade compete with $OxyB_{tei}$ for the X-domain binding site during an in vitro activity assay: turnover reactions were performed under single turnover conditions (1.2-fold molar excess of $OxyB_{tei}$ over **1**-L-PCP-X) in either the presence or absence of additional Oxy enzymes ($OxyA_{tei}$ or $OxyC_{tei}$). The highest cross-linking activity for $OxyB_{tei}$ was observed in the absence of a second P450, whereas in the presence of $OxyA_{tei}$ or $OxyC_{tei}$ the formation of **2** was reduced to approximately one-third of the original levels (Figure 6, middle, SI Table S4). Prior incubation of the **1**-L-PCP-X with either $OxyA_{tei}$ or $OxyC_{tei}$ led to further decrease in the amount of **2** detected (Figure 6, right); this competition effect can be counteracted to some extent by the incubation of $OxyB_{tei}$ with the **1**-L-PCP-X substrate prior to the addition of a competing Oxy (Figure 6, left). Under these single turnover conditions, no second ring closure was observed either for the reaction containing $OxyC_{tei}$ (shown to be catalytically incompetent in vitro)[22] or for $OxyA_{tei}$. These results show that subsequent P450s in the pathway are able to compete with $OxyB_{tei}$ for the same P450 interaction interface on the **1**-L-PCP-X protein irrespective of the cross-linking state of the bound peptide.

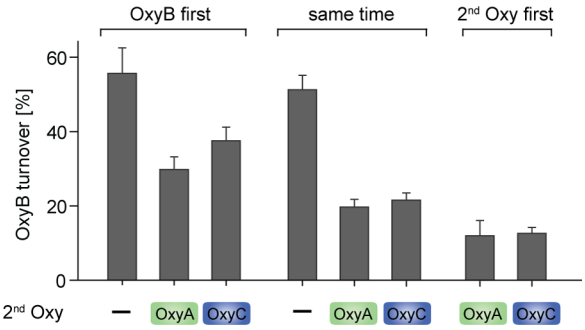

Figure 6. P450 competition experiment. Investigation of the competition of the teicoplanin P450s ($OxyB_{tei}$, $OxyA_{tei}$, $OxyC_{tei}$) for the X-domain binding interface by monitoring the $OxyB_{tei}$ cross-linking activity toward linear **1**-L-PCP-X_{tei}.

Implications for the Reaction Mechanism. Our results raise two further questions: what is the mechanism that triggers the exchange of the P450s on the X-domain binding interface and how do these P450s distinguish between the different, albeit structurally very similar, substrate peptides?

Consistent with the oxidation order, we have shown that the cognate substrate induces a stronger spectral response in the respective P450 enzyme. However, in terms of binding affinities no clear difference can be observed between $OxyB_{tei}$ and $OxyA_{tei}$ for **1**-L-PCP-X, which indicates that the cross-linking state most likely does not actively trigger the exchange of the P450 on the X-domain. Due to experimental difficulties it is not possible to quantify the K_D value of the monocyclic product **2**-L-PCP-X to $OxyB_{tei}$. However, the progression curves of the steady state kinetics for $OxyB_{tei}$ (SI Figure S8) demonstrate a gradual decrease in reaction velocity commencing at ~25% product formation, which is likely caused by a combination of substrate depletion and product inhibition. On the basis of the slope of this slower phase at about 35% progression of the reaction, we can estimate that the K_D for the product is in the same order of magnitude as the K_D for the substrate (SI Supplementary Note).

Furthermore, our combined data for $OxyB_{tei}$ substrate binding and turnover indicate that the K_M is at least 3-fold smaller than the K_D for the linear **1**-L-PCP-X, which helps to increase specificity and to reduce product inhibition. Such a K_M/K_D-relationship has been described for mechanisms involving multiple reaction intermediates that accumulate as a consequence of a partially rate limiting final or late step in the reaction.[38,39] Prominent examples include epoxide hydrolases[40] and DNA-polymerases:[41,42] in the latter, the mechanism for substrate selection also involves structural changes within the polymerase that depend on the respective ligand.

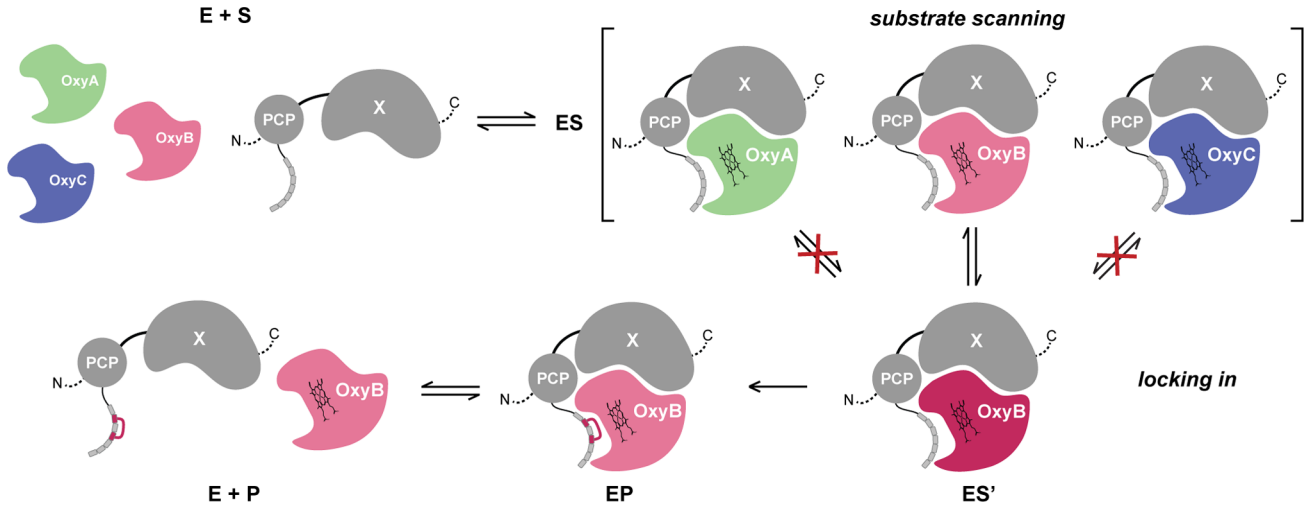

Figure 7. Suggested model for peptide cyclization in GPA biosynthesis: P450 recruitment to the peptide and recognition of the peptide cyclization state by the P450 (substrate scanning; reported by the K_D value) followed by an induced conformational change of the enzyme (locking in), catalysis and product release; the K_M value is representative for substrate affinity in steady-state of the entire reaction cycle up to the rate limiting step.

DOI: 10.1021/jacs.6b00307
J. Am. Chem. Soc. 2016, 138, 6746–6753

On the basis of the similarity of our findings for $OxyB_{tei}$ substrate binding and turnover to these well-studied systems, we hypothesize that $OxyB_{tei}$ undergoes a specific transformation upon binding of the correct substrate. This effect must follow the displacement of the axial water observed by UV−visible spectroscopy and would serve to enhance the affinity for the substrate or reaction intermediate.[38] Possible sources for such a transformation include minor rearrangements in the active site (e.g., needed to establish a water network to support the reaction pathway or to facilitate electron transfer) or larger rearrangements of secondary structural elements; this includes possible changes caused by the interaction with the redox partners initialized through the binding of the correct substrate. The data also suggest that one of the last catalytic steps of the reaction is a slow process:[38] this could well be the second electron transfer step, which has been shown to be at least partially rate-limiting in other P450 systems.[43] However, the reported rates for the second electron transfer step vary widely from >100 s^{-1} for a class I redox system to 8.4−0.37 s^{-1} described for a class II microsomal system.[43] Hence, only in an extreme case would this reaction step be potentially rate limiting in the $OxyB_{tei}$-catalyzed reaction with a rate of 0.16 s^{-1} measured for the complete catalytic cycle. The protein−protein interaction driving the P450 recruitment process also needs to be considered in assigning the possible source of the slow step, and leads us to favor product release as the rate-limiting step in the reaction.

On the basis of these considerations, our proposed reaction scheme for $OxyB_{tei}$ − that should be deemed an initial working model−involves the following steps (Figure 7): initial recruitment of $OxyB_{tei}$ to the *peptidyl*-PCP-X, which is mediated by protein−protein interactions and the binding of the peptide to the active site of $OxyB_{tei}$ that is characterized by a spin state shift of the heme iron (ES); a conformational change in $OxyB_{tei}$ triggered by the recognition of the appropriate cross-linking state of the peptide (ES′); and last the formation (EP) and release of the monocyclic product (E+P). This proposed mechanism enables us to rationalize both the K_M being smaller than the K_D for the natural substrate peptide and the rather moderate product inhibition in our activity assays, given that the affinities of the product and substrate are actually in a similar range; in vivo this mechanism may be relevant to ensure the correct initiation of the peptide cyclization process and—assuming that this mechanism is not only restricted to OxyB but also applies to the following oxygenases—the efficient progression of the oxygenation cascade.

CONCLUSIONS

In this study we performed a quantitative investigation of the regulation of the peptide-cyclization cascade in GPA biosynthesis. We showed that the peptide tailoring P450s are recruited to the same binding site on the X-domain surface in the terminal NRPS module. In spite of their inability to turn over peptides with the incorrect cyclization state, these P450 enzymes directly compete for the X-domain binding site even in the presence of nonsubstrate peptides. By determining the kinetic parameters of $OxyB_{tei}$-catalyzed turnover and comparing them to the affinities determined for substrates and products, we propose a reaction model that involves one or more intermediates of the enzyme−substrate complex prior to catalysis and product release. In our model this translates to a continuous association/dissociation of P450s (scanning) with the NRPS. This occurs with similar binding affinities independent of the peptide cross-linking state, until one P450 binds to its cognate substrate (e.g., OxyB−linear peptide, OxyA−monocyclic peptide) and undergoes a conformational change that increases its affinity for the substrate (locking in): this serves to drive the reaction forward. The reaction product can then dissociate as the substrate for the next P450 in the cascade. This proposed mechanism relies on the ability of the X-domain to randomly interact with tailoring P450s and the ability of the P450s to discriminate between cyclization states of the NRPS-bound peptides, which we have confirmed. In order to prevent this process from dramatically slowing the rate of aglycone formation, the tailoring cascade would need to be faster than the NRPS assembly line. However, since a GPA producing NRPS has not been kinetically characterized to date, we are not able to directly compare the k_{cat} of $OxyB_{tei}$ to the preceding catalytic steps. The only available kinetic parameters are those of the A-domain in the reconstituted Tcp10 module (third module in teicoplanin NRPS; ∼2 min^{-1}),[44] showing that $OxyB_{tei}$ is about 5-fold faster. Furthermore, the characterization of other NRPS and PKS machineries suggests that the precursor assembly proceeds at similar rates as observed for Tcp10 (k_{cat}: pyochelin NRPS ∼2 min^{-1},[45] yersinibactin NRPS/PKS hybrid ∼1.4 min^{-1},[46] 6-deoxyerythronolide B PKS 1 min^{-1}).[47] Therefore, we suggest that the oxidative modifications in *trans* are faster than the peptide assembly itself, allowing the efficient tailoring of GPA peptides. Additionally, related questions still remain to be answered, including whether the thioesterase domain also competes for the *peptidyl*-PCP in the terminal module and if the specificity of the Te-domain ultimately determines the timing of events by acting as a logic gate for the release of fully cyclized GPA aglycones in a manner that has been suggested for other Te-domains.[12,45,48] These questions will need to be addressed in order to build a complete picture of the interplay of NRPS and P450s in the final steps of GPA biosynthesis.

MATERIALS AND METHODS

For detailed experimental procedures refer to Supporting Information.

Peptide Synthesis. The synthesis and characterization of the heptapeptide-CoA conjugates (**1**-D/L-CoA, H_2N-D-Hpg_1-D-Tyr_2-L-Hpg_3-D-Hpg_4-D-Hpg_5-L-Tyr_6-D/L-Hpg_7-SCoA and **4**-D/L-CoA, H_2N-D-Leu_1-D-Tyr_2-L-Asn_3-D-Hpg_4-D-Hpg_5-L-Tyr_6-L/D-Hpg_7-SCoA) was performed as previously described.[49,23] For separation of the diastereomers of the teicoplanin-related peptide, preparative HPLC was performed yielding the CoA-peptides **1**-L-CoA and **1**-D-CoA (0−3 min 10% ACN in H_2O + 0.1% formic acid, 3−33 min up to 30% ACN in H_2O + 0.1% formic acid, flow rate 20.0 mL/min Waters XBridge BEH300 Prep C18 column (5 μm, 19 × 150 mm)). The isolated CoA-peptides were characterized by HRMS and NMR-spectroscopy (see Supporting Information). The quantity of peptide substrates required for the experiments contained in this work necessitated the use of several different peptide batches. This contributed to some variability within the experiments, reflected in the stated standard errors and deviations of the extrapolated parameters.

Protein Expression and Purification. The plasmids encoding NRPS proteins comprise a natural fusion of the PCP- and X-domain from module seven of the teicoplanin (Tcp12, Uniprot protein ID: Q70AZ6, PCP-X_{tei}) and vancomycin (VpsC, Uniprot protein ID: G4V4R2, PCP-X_{van}) producing NRPS as previously described.[22,23] The proteins were expressed under the control of a T7 promoter in the *E. coli* BL21Gold (DE3) strain (Agilent, Waldbronn, Germany) and purified as previously described for PCP7 proteins.[50] The plasmids encoding the P450 enzymes involved in teicoplanin ($OxyB_{tei}$ (Uniprot protein ID: Q70AY8), $OxyA_{tei}$ (Uniprot protein ID: Q6ZZI8), $OxyC_{tei}$ (Uniprot protein ID: Q70AY6)) and vancomycin ($OxyB_{van}$ (Uniprot protein ID: G4V4R5)) biosynthesis were generated and described

DOI: 10.1021/jacs.6b00307
J. Am. Chem. Soc. 2016, 138, 6746−6753

previously.[22,23,50] The genes were expressed under the control of a T7 promoter in the *E. coli* KRX strain (Promega GmbH, Mannheim, Germany) and purified as described by Haslinger et al. 2014 for $OxyB_{tei}$.[50] The redox partners for the in vitro P450 turnover assay were obtained from Dr. Stephen Bell (Adelaide, Australia).[51]

Analytical Size Exclusion Chromatography. $OxyA_{tei}$ and $OxyC_{tei}$ were incubated with the different PCP-X_{tei} variants in a 1:3 mixture (Oxy: 33 μM, PCP-X_{tei} variant: 100 μM) for 30 min at RT in a final volume of 100 μL (50 mM Tris/HCl pH 7.4, 100 mM NaCl). The samples were analyzed via analytical size exclusion chromatography (aSEC) with a Superose-12 10/300 GL column (GE Healthcare, Munich, Germany) connected to an HPLC system (Waters GmbH, Eschborn, Germany) with online absorption detection at 280 and 415 nm (Waters).

Loading of *Peptidyl*-CoA onto *apo*-PCP-X Proteins. Heptapeptide-CoA conjugates were loaded onto *apo*-PCP-X proteins as previously described.[22,25] Following the reaction the excess of unbound peptide was removed by a dilution-concentration procedure using centrifugal filter units with a 10 000 MW cutoff (Merck Millipore, Darmstadt, Germany) and low salt buffer (50 mM Hepes pH 7.0, 50 mM NaCl for turnovers and 20 mM Hepes pH 7.0, 50 mM NaCl for UV−visible spectroscopy; 4× 1:5 dilution). The *peptidyl*-PCP-X proteins were directly used for UV−visible spectroscopic measurements and the P450 in vitro activity assays.

Standard P450 Activity Assay. For in vitro cross-linking activity of $OxyB_{tei}$, 50 μM *peptidyl*-PCP-X was added to the turnover reaction mix containing 2 μM $OxyB_{tei}$, the palustrisredoxin B variant A105V (PuxB)/ palustrisredoxin reductase (PuR) redox system in 5:1:50 ratio (PuxB:PuR:*peptidyl*-PCP-X) and the glucose dehydrogenase/glucose NADH regeneration system (0.033 mg/mL, 0.33%, respectively) in low salt buffer (50 mM Hepes pH 7.0, 50 mM NaCl). The reaction was started by adding 2 mM NADH, and after incubation for 1 h at 30 °C with gentle shaking the reaction was stopped by addition of methylamine (40% methylamine in water) in a 32 000 molar excess over the *peptidyl*-PCP-X, resulting in the cleavage of the thioester. After incubation for 15 min at RT the reaction was neutralized with diluted formic acid and the cleaved peptides were purified via solid phase extraction (Strata-X polymeric reversed phase, Phenomenex, Aschaffenburg, Germany). Peptides were analyzed by analytical HPLC-MS (gradient: 0−4 min 5% solvent B (ACN in H_2O + 0.1% formic acid), 4−4.5 min up to 15% solvent B, 4.5−25 min up to 50% solvent B; Waters XBridge BEH 300 C_{18}, 5 μm, 4.6 × 250 mm, flow rate 1.0 mL/min) using single ion monitoring in negative mode. The coupled $OxyB_{tei}$ and $OxyA_{tei}$ turnover reaction was performed under standard conditions, additionally containing 2 μM of $OxyA_{tei}$.

UV−Visible Spectroscopy. For binding of monocyclic substrate peptides to P450s, *peptidyl*-PCP-X was subjected to $OxyB_{tei}$-mediated cyclization in a modified turnover protocol (see SI). The monocyclic and linear *peptidyl*-PCP-X conjugates were concentrated to 200−600 μM as determined by the method of Ehresmann et al.[52] and immediately used for titrations. The complete removal of NADH in the monocyclic probes was confirmed by measuring the absorption at λ = 340 nm. For the titrations solutions of 2.2 μM $OxyB_{tei}$, 2.3 μM $OxyA_{tei}$ or 1.3 μM $OxyB_{van}$ were prepared in low salt buffer (20 mM Hepes pH 7.0, 50 mM NaCl), split into two quartz cuvettes (sample and reference, 490 μL) and placed into a Jasco V-650 double beam spectrophotometer equilibrated to 30 °C. After blanking, the baseline was recorded for λ = 350−600 nm. The ligand was added stepwise and spectra were recorded after a 1 min equilibration. The amplitudes of the spectra were extrapolated ($\Delta Abs = A_{max} - A_{min}$), plotted against the ligand concentration and fitted with the quadratic equation ($Y = (\Delta Abs_{max} - \Delta Abs_0) \times ([titrand] - 0.5 \times (-K_D + [titrand][P450] + sqrt(4 \times K_D \times [titrand] + (K_D - [titrand] + [P450])^2)))/[P450] + \Delta Abs_0$). Since it was not possible to separate the linear and the monocyclic *peptidyl*-PCP-X after the turnover reaction, the actual OxyB turnover yields in the reported substrate concentrations were considered for the titrations.

For displacement studies, increasing amounts of *apo*- or *holo*-PCP-X or X-domain were added in a stepwise manner to a preformed complex of $OxyB_{tei}$ and **1**-L-PCP-X (2.5, 5, or 10 μM of **1**-L-PCP-X) while the decrease in spectral response of $OxyB_{tei}$ was monitored, indicative of the displacement of **1**-L-PCP-X from $OxyB_{tei}$. The resulting data sets were analyzed in a global data analysis by DynaFit4[37] based on a single site, one step binding model (see Supporting Information).

Kinetic Studies. Kinetic parameters for the OxyB homologues ($OxyB_{tei}$ and $OxyB_{van}$) were obtained by recording various time points of the enzymatic turnover (10 or 15 s time interval) at varying concentrations of *peptidyl*-PCP-X substrate (0.31−30 μM). The reactions were performed in the standard turnover mix as described above ($c(OxyB_{tei})$ = 62.5 nM, $c(OxyB_{van})$ = 31.3 nM). After initial incubation at 30 °C, the reactions were started through the addition of NADH and the OxyB enzyme, stopped by pipetting 105 μL of the reaction into 15 μL methylamine solution (40% methylamine in water) and further treated and analyzed as described above. To cover a broad range of substrate concentrations, some assay parameters were adjusted for low substrate concentrations (substrate range 0.31−1.25 μM): OxyB concentrations were reduced to 31.3 nM ($OxyB_{tei}$) and 15.6 nM ($OxyB_{van}$) with the resulting data points normalized to the enzyme concentration; the reaction volume was increased from 105 to 315 μL per time point to yield enough material for the HPLC-MS analysis; the time interval between sampling was decreased from 15 to 10 s to ensure proper coverage of the initial velocity phase. The redox system composed of PuxB and PuR was used in an excess over the OxyB with replicates obtained from experiments performed with different concentration ratios between the P450 and the redox partners (OxyB:PuxB:PuR) with 1:10:2, 1:20:10 and 1:40:20 for $OxyB_{tei}$ and 1:40:20 and 1:80:40 for $OxyB_{van}$. Independent of varying the concentrations of the redox system, all measurements showed comparable results. This indicates that the initial velocity of the reaction is not limited by electron transfer from the redox system under the chosen experimental conditions.

P450 Competition Experiment. In the P450 competition experiments the $OxyB_{tei}$ (3 μM) activity toward **1**-L-PCP-X was monitored in the presence and absence of one additional Oxy (3 μM of $OxyA_{tei}$ or $OxyC_{tei}$) under single turnover conditions (1.2-fold molar excess of $OxyB_{tei}$ over substrate). The reactions were performed with 2.5 μM of **1**-L-PCP-X in 50 mM Hepes pH 7.0, 50 mM NaCl additionally containing the Oxys, PuxB and PuR in a ratio of (1:2.5:0.5) and the NADH regeneration system. The redox partners and regeneration systems were always incubated at 30 °C prior to the reaction. Depending on the experimental setup, a mix of the competing P450 and the substrate, $OxyB_{tei}$ and the substrate or the substrate alone (incubated for 30 min, RT) were then added to the mix and incubated for 30 s. Then the second P450 was added ($OxyB_{tei}$, competing P450s or $OxyB_{tei}$ together with competing P450, respectively) and after 10 s the reaction was started by adding 2 mM NADH, stopped after 5s using methylamine and further treated as described above.

■ ASSOCIATED CONTENT

Supporting Information

The Supporting Information is available free of charge on the ACS Publications website at DOI: 10.1021/jacs.6b00307.

Chemical analysis of substrates, detailed experimental procedures, supporting results including raw data. (PDF)

■ AUTHOR INFORMATION

Corresponding Author

*max.cryle@monash.edu

Present Address

[‖]Department of Chemical Engineering, Massachusetts Institute of Technology, 77 Massachusetts Avenue, Cambridge, Massachusetts 02139, United States.

Author Contributions

[#]M.P. and K.H. contributed equally.

DOI: 10.1021/jacs.6b00307
J. Am. Chem. Soc. 2016, 138, 6746−6753

Notes

The authors declare no competing financial interest.

■ ACKNOWLEDGMENTS

The authors are grateful to Dr. Stephen Bell for provision of the plasmids encoding the redox proteins, Melanie Müller for mass spectral analysis and Chris Roome for IT support. This work was supported by the Deutsche Forschungsgemeinschaft (Emmy-Noether Program, CR 392/1−1 granted to MJC). M.J.C. also acknowledges the support of Monash University and the EMBL Australia program.

■ REFERENCES

(1) Nicolaou, K. C.; Boddy, C. N. C.; Bräse, S.; Winssinger, N. *Angew. Chem., Int. Ed.* **1999**, *38*, 2096−2152.
(2) Hamed, R. B.; Gomez-Castellanos, J. R.; Henry, L.; Ducho, C.; McDonough, M. A.; Schofield, C. J. *Nat. Prod. Rep.* **2013**, *30*, 21−107.
(3) Marahiel, M. A. *J. Pept. Sci.* **2009**, *15*, 799−807.
(4) Hur, G. H.; Vickery, C. R.; Burkart, M. D. *Nat. Prod. Rep.* **2012**, *29*, 1074−1098.
(5) Mootz, H. D.; Schwarzer, D.; Marahiel, M. a. *ChemBioChem* **2002**, *3*, 490−504.
(6) Wohlleben, W.; Mast, Y.; Muth, G.; Röttgen, M.; Stegmann, E.; Weber, T. *FEBS Lett.* **2012**, *586*, 2171−2176.
(7) Al Toma, R. S.; Brieke, C.; Cryle, M. J.; Süssmuth, R. D. *Nat. Prod. Rep.* **2015**, *32*, 1207−1235.
(8) Samel, S. A.; Marahiel, M. A.; Essen, L.-O. *Mol. BioSyst.* **2008**, *4*, 387−393.
(9) Luo, L.; Kohli, R. M.; Onishi, M.; Linne, U.; Marahiel, M. A.; Walsh, C. T. *Biochemistry* **2002**, *41*, 9184−9196.
(10) Labby, K. J.; Watsula, S. G.; Garneau-Tsodikova, S. *Nat. Prod. Rep.* **2015**, *32*, 641−653.
(11) Pang, B.; Wang, M.; Liu, W. *Nat. Prod. Rep.* **2016**, *33*, 162−173.
(12) Horsman, M. E.; Hari, T. P. A.; Boddy, C. N. *Nat. Prod. Rep.* **2016**, *33*, 183−202.
(13) Yim, G.; Thaker, M. N.; Koteva, K.; Wright, G. *J. Antibiot.* **2014**, *67*, 31−41.
(14) Butler, M. S.; Hansford, K. A.; Blaskovich, M. A. T.; Halai, R.; Cooper, M. A. *J. Antibiot.* **2014**, *67*, 631−644.
(15) Stegmann, E.; Frasch, H. J.; Wohlleben, W. *Curr. Opin. Microbiol.* **2010**, *13*, 595−602.
(16) Felnagle, E. A.; Jackson, E. E.; Chan, Y. A.; Podevels, A. M.; Berti, A. D.; McMahon, M. D.; Thomas, M. G. *Mol. Pharmaceutics* **2008**, *5*, 191−211.
(17) Hadatsch, B.; Butz, D.; Schmiederer, T.; Steudle, J.; Wohlleben, W.; Süssmuth, R. D.; Stegmann, E. *Chem. Biol.* **2007**, *14*, 1078−1089.
(18) Bischoff, D.; Bister, B.; Bertazzo, M.; Pfeifer, V.; Stegmann, E.; Nicholson, G. J.; Keller, S.; Pelzer, S.; Wohlleben, W.; Süssmuth, R. D. *ChemBioChem* **2005**, *6*, 267−272.
(19) Bischoff, D.; Pelzer, S.; Bister, B.; Nicholson, G. J.; Stockert, S.; Schirle, M.; Wohlleben, W.; Jung, G.; Süssmuth, R. D. *Angew. Chem., Int. Ed.* **2001**, *40*, 4688−4691.
(20) Zerbe, K.; Woithe, K.; Li, D. B.; Vitali, F.; Bigler, L.; Robinson, J. A. *Angew. Chem., Int. Ed.* **2004**, *43*, 6709−6713.
(21) Woithe, K.; Geib, N.; Zerbe, K.; Dong, B. L.; Heck, M.; Fournier-Rousset, S.; Meyer, O.; Vitali, F.; Matoba, N.; Abou-Hadeed, K.; Robinson, J. A. *J. Am. Chem. Soc.* **2007**, *129*, 6887−6895.
(22) Haslinger, K.; Peschke, M.; Brieke, C.; Maximowitsch, E.; Cryle, M. J. *Nature* **2015**, *521*, 105−109.
(23) Brieke, C.; Peschke, M.; Haslinger, K.; Cryle, M. J. *Angew. Chem., Int. Ed.* **2015**, *54*, 15715−15719.
(24) Sunbul, M.; Marshall, N. J.; Zou, Y.; Zhang, K.; Yin, J. *J. Mol. Biol.* **2009**, *387*, 883−898.
(25) Brieke, C.; Kratzig, V.; Haslinger, K.; Winkler, A.; Cryle, M. J. *Org. Biomol. Chem.* **2015**, *13*, 2012−2021.
(26) Schmartz, P. C.; Wölfel, K.; Zerbe, K.; Gad, E.; El-Tamany, E. S.; Ibrahim, H. K.; Abou-Hadeed, K.; Robinson, J. A. *Angew. Chem., Int. Ed.* **2012**, *51*, 11468−11472.
(27) Woithe, K.; Geib, N.; Meyer, O.; Wörtz, T.; Zerbe, K.; Robinson, J. A. *Org. Biomol. Chem.* **2008**, *6*, 2861−2867.
(28) Stegmann, E.; Pelzer, S.; Bischoff, D.; Puk, O.; Stockert, S.; Butz, D.; Zerbe, K.; Robinson, J.; Süssmuth, R. D.; Wohlleben, W. *J. Biotechnol.* **2006**, *124*, 640−653.
(29) Bischoff, D.; Pelzer, S.; Holtzel, A.; Nicholson, G. J.; Stockert, S.; Wohlleben, W.; Jung, G.; Süssmuth, R. D. *Angew. Chem., Int. Ed.* **2001**, *40*, 1693−1696.
(30) Süssmuth, R. D.; Pelzer, S.; Nicholson, G.; Walk, T.; Wohlleben, W.; Jung, G. *Angew. Chem., Int. Ed.* **1999**, *38*, 1976−1979.
(31) Uhlmann, S.; Süssmuth, R. D.; Cryle, M. J. *ACS Chem. Biol.* **2013**, *8*, 2586−2596.
(32) Haslinger, K.; Brieke, C.; Uhlmann, S.; Sieverling, L.; Süssmuth, R. D.; Cryle, M. J. *Angew. Chem., Int. Ed.* **2014**, *53*, 8518−8522.
(33) Cryle, M. J.; Meinhart, A.; Schlichting, I. *J. Biol. Chem.* **2010**, *285*, 24562−24574.
(34) Chen, H.; Walsh, C. T. *Chem. Biol.* **2001**, *8*, 301−312.
(35) Cryle, M. J.; Schlichting, I. *Proc. Natl. Acad. Sci. U. S. A.* **2008**, *105*, 15696−15701.
(36) Chen, H.; Hubbard, B. K.; O'Connor, S. E.; Walsh, C. T. *Chem. Biol.* **2002**, *9*, 103−112.
(37) Kuzmic, P. *Anal. Biochem.* **1996**, *237*, 260−273.
(38) Fersht, A. The basic equations of enzyme kinetics. In *Structure and Mechanism in Protein Science*, 2nd ed.; W H Freeman: New York, 1999; pp 103−131.
(39) Gutfreund, H. *Kinetics for the Life Sciences: Receptors, Transmitters and Catalysts*; Cambridge University Press: Cambridge, 1995.
(40) Johnson, W. W.; Yamazaki, H.; Shimada, T.; Ueng, Y. F.; Guengerich, F. P. *Chem. Res. Toxicol.* **1997**, *10*, 672−676.
(41) Tsai, Y.-C.; Johnson, K. A. *Biochemistry* **2006**, *45*, 9675−9687.
(42) Johnson, K. A. *Biochim. Biophys. Acta, Proteins Proteomics* **2010**, *1804*, 1041−1048.
(43) Denisov, I. G.; Sligar, S. G. *Cytochrome P450: Structure, Mechanism, and Biochemistry*, 4th ed.; De Montellano, P. R. O., Ed.; Springer: Berlin, 2015; pp 69−109.
(44) Kittilä, T.; Schoppet, M.; Cryle, M. J. *ChemBioChem* **2016**, *17*, 576−584.
(45) Patel, H. M.; Walsh, C. T. *Biochemistry* **2001**, *40*, 9023−9031.
(46) Miller, D. A.; Luo, L.; Hillson, N.; Keating, T. A.; Walsh, C. T. *Chem. Biol.* **2002**, *9*, 333−344.
(47) Lowry, B.; Robbins, T.; Weng, C.-H.; O'Brien, R. V.; Cane, D. E.; Khosla, C. *J. Am. Chem. Soc.* **2013**, *135*, 16809−16812.
(48) Gaudelli, N. M.; Townsend, C. A. *Nat. Chem. Biol.* **2014**, *10*, 251−258.
(49) Brieke, C.; Cryle, M. J. *Org. Lett.* **2014**, *16*, 2454−2457.
(50) Haslinger, K.; Maximowitsch, E.; Brieke, C.; Koch, A.; Cryle, M. J. *ChemBioChem* **2014**, *15*, 2719−2728.
(51) Bell, S. G.; Xu, F.; Johnson, E. O. D.; Forward, I. M.; Bartlam, M.; Rao, Z.; Wong, L. L. *JBIC, J. Biol. Inorg. Chem.* **2010**, *15*, 315−328.
(52) Ehresmann, B.; Imbault, P.; Well, J. H. *Anal. Biochem.* **1973**, *54*, 454−463.

DOI: 10.1021/jacs.6b00307
J. Am. Chem. Soc. 2016, 138, 6746−6753